

# Studies on stellar rotation

## I. The theoretical apsidal motion for evolved rotating stars

A. Claret

Instituto de Astrofísica de Andalucía, CSIC, Apartado 3004, E-18080 Granada, Spain

Received 1 June 1999 / Accepted 3 August 1999

**Abstract.** The quasi-spherical approximation, with some modifications, was implemented in our stellar evolution code to take into account the effect of rotation on the internal structure of the stars and, in particular, on the apsidal motion constant. Three models with masses 2, 7 and 15  $M_{\odot}$  were used since they are representative of the mass range where apsidal motion is detected in binary stars. We adopted two limiting cases of angular momentum redistribution: local conservation and rigid body rotation. It was found that the influence of rotation on internal structure depends strongly on the distortion of the configuration characterized by the parameter  $\lambda = 2v^2/(3gR)$  at the surface of the model. Such results make the work of introducing the correction for rotation in the apsidal motion analysis an easier task since it is sufficient to decrease the theoretical  $\log k_2$  by 0.87  $\lambda_s$ .

**Key words:** stars: binaries: eclipsing – stars: evolution – stars: interiors – stars: rotation

### 1. Introduction

Apsidal motion is an important and complementary test to stellar evolution theory. In fact, before directly comparing the theoretical apsidal motion rates with observations, a stellar model has to pass several previous tests as isochrones, masses, radius, effective temperatures, etc. The first calculations of the apsidal motion constants were performed by Schwarzschild (1958) and Kopal (1965). They noticed that the theoretical values of  $k_2$  were systematically larger than those obtained observationally. This means that the real stars seemed to be more mass concentrated than predicted by the models. This trend persisted during several decades. At that time the discrepancies were of the order of 300%. As the earlier stellar models were homogeneous some investigations were directed towards evolved models, searching for a possible explanation of the discrepancies (Mathis 1967, Semeniuk & Paczynsky 1968, Cisneros-Parra 1970, Koch 1972, Petty 1973). Even for more modern models (Hejlesen 1987) that tendency still remained.

More recently Claret & Giménez (1992, 1993) and Claret 1995, in a series of papers on stellar models and internal struc-

ture, were able to reduce the discrepancies at acceptable levels for systems whose relativistic contributions were small. Using new opacities provided by the Lawrence Livermore Group (Rogers & Iglesias 1992, Iglesias et al. 1992) and moderate core overshooting these authors showed that a great part of the discrepancies were due to the input physics of the models.

For some few problematic cases the discrepancies were still larger, mainly for DI Her, AS Cam and V541 Cyg. As the relativistic contribution to the apsidal motion of such stars is important, one of the possible solutions of the problem would be a revision of the gravitation theory (Moffat, 1984, 1989). However, as shown by Claret (1997) the predictions of the General Relativity together with the predictions of recent stellar models were able to explain the relativistic and non relativistic systems. No alternative gravitation theory seems to be needed. In a separate paper Claret (1998, 1999) investigated the cases of the three mentioned systems. As a revision of the gravitation theory may be discarded, he proposed an explanation based on the difference between the intervals of time involved (observations and apsidal motion period) and on the position of the periastron angle. Of course, an hypothesis like the third body is also probable but it needs an observational confirmation. Apart from these few problematic systems which were investigated in the quoted papers, the comparison between theory and observation of apsidal motion indicates that we are now dealing with refinements both in theory and observations.

As concerns rotation specifically, the correction in the theoretical  $k_2$  is not expected to be too large, at least for systems not excessively distorted. As the discrepancies decreased very much with the improvements in the stellar models and in the observations, the effect of rotation, though small, becomes important. About 25 years ago Stothers (1974) showed that for homogeneous configurations the rotation affects the internal structure and, in particular, the apsidal motion constant  $k_2$ . Uniform rotation was considered and the method developed by Faulkner et al. (1968) was applied. The main result was that the correction due to rotation would be  $-0.7 \lambda$  where  $\lambda$  is  $2v^2/(3gR)$ ,  $v$  being the rotational velocity,  $g$  the gravity and  $R$  the radius.

Claret & Giménez (1993) used a simple version of the method by Kippenhan & Thomas (1970), hereafter KT, in order to evaluate the effects of rotation on the internal stellar structure. These authors also used ZAMS models and they found results

similar to Stother's for realistic values of the rotational velocities. However, the changes of the stellar parameters caused by evolution and rotation and the transport of angular momentum could change the above relationship. In order to investigate such a possibility, evolved stellar models with rotation are computed and the results are compared with standard ones.

In Sect. 2 the numerical method to introduce rotation is explained. Sect. 3 is dedicated to analyze the results and draw some conclusions.

## 2. The calculation of $f_P$ and $f_T$

The basic properties of the standard (without rotation) evolution code are described in Claret 1995. In order to consider rotation we have used the KT formalism with some modifications. In our previous work (Claret & Giménez 1993) we adopted for the rotating model the configuration of the Roche model. Such an approximation means that the integral that describes the distortion contribution to the total potential is ignored. In that case the surface value of  $\eta_2$  is equal to 3 (infinite mass concentration). Although these approximations in some cases are good, in the present paper we decided to consider the three contributions to the potential: the spherically symmetric gravitational potential, that due to rotation and that which describes the distortion contribution.

We restricted the calculation to first order theory. Thus the total potential can be written as (Kopal 1959)

$$\psi = \frac{GM_\psi}{r^2} + \frac{1}{2}\Omega^2 r^2 \sin^2 \theta - \frac{4\pi G}{5r^3} P_2(\cos \theta) \int_0^a \rho \frac{d}{da'} (a'^5 f_2) da' \quad (1)$$

where

$$r = a(1 - f_2 P_2(\cos \theta)) \quad (2)$$

$$f_2 = \frac{5\Omega^2 a^3}{3GM_\psi(2 + \eta_2)} \quad (3)$$

$\Omega$  is the angular velocity,  $P_2(\cos \theta)$  is the second Legendre polynomial,  $a$  the radius of the level surface,  $\eta_2$  is connected with Radau's equation, and the remaining symbols have their usual meaning.

The differential equations of the structure are changed as follows:

$$\frac{\partial r_\psi}{\partial M_\psi} = \frac{1}{4\pi\rho r_\psi^2} \quad (4)$$

$$\frac{\partial P_\psi}{\partial M_\psi} = -\frac{GM_\psi}{4\pi r_\psi^4} f_P \quad (5)$$

$$\frac{\partial L_\psi}{\partial M_\psi} = \epsilon - T \frac{\partial S}{\partial t} \quad (6)$$

$$\frac{\partial \ln T_\psi}{\partial \ln P_\psi} = \frac{3\kappa L_\psi P_\psi f_T}{16\pi a c G M_\psi T_\psi^4 f_P} \quad (7)$$

and the Schwarzschild criterion is given by:

$$\frac{\partial \ln T_\psi}{\partial \ln P_\psi} = \min[\nabla_{ad}, \nabla_{rad} \frac{f_T}{f_P}] \quad (8)$$

where  $\nabla_{ad}$  and  $\nabla_{rad}$  are the spherical adiabatic and radiative gradients. Some modes of convective motions may be inhibited by rotation but in the present paper we do not take into account these effects and the conventional criterion of stability is used (Randers 1942). The quantities  $f_P$  and  $f_T$  are given by

$$f_P = 4\pi r_\psi^4 \frac{1}{GM_\psi S_\psi g^{-1}} \quad (9)$$

and

$$f_T = \left( \frac{4\pi r_\psi^2}{S_\psi} \right)^2 \frac{1}{\bar{g} g^{-1}} \quad (10)$$

where the mean values of  $g$  and  $g^{-1}$  are taken over equipotentials.

To compute  $f_P$  and  $f_T$  one has to know the relationship between  $a$  and  $r_\psi$ . The radius of a sphere with equivalent volume is related to the radius of the level surface by

$$r_\psi^3 = a^3 \left( 1 + \frac{3}{5} f_2^2 - \frac{2}{35} f_2^3 \right) \quad (11)$$

The value of  $a$  is obtained through iteration of Eq. 11.

In principle, we would need to integrate simultaneously Radau's equation to obtain  $\eta_2$  at each point of the model. A similar procedure should also be performed to evaluate the integral that appears in Eq. 1 and that will appear in the definition of the local gravity  $-\frac{d\psi}{dn}$  – and also its inverse. Endal & Sofia 1976 used the ratio  $\bar{\rho}/\rho_c$  to evaluate  $\eta_2$  as a function of the polytropic index. We have introduced an alternative way: the first model is computed without rotation. It will give, through integrations, the values of  $\eta_2$  and of the integral for each point to be used in a second model which includes rotation. For this second model and all following ones the values of the integral and of  $\eta_2$  include the effects for rotation. The model  $n$  will be computed considering the values of the integral and of  $\eta_2$  as derived from the model  $n-1$ . Provided that neighboring models have no large differences in their structures the method gives a good accuracy. This can be obtained by controlling the time steps. In addition to the required accuracy, this method does not need to divide the star in two parts since the values of  $\eta_2$  and of the integral are always evaluated directly from the center up to the atmosphere. The local gravity and its inverse are calculated by derivating Eq. 1 with respect to  $r$  and  $\theta$ . Their mean values are computed using Gauss quadrature over the equipotentials. Numerical tests reveal that 10 points are sufficient if one desires a compromise between accuracy and speed of calculation.

The only boundary condition affected by rotation is that for the atmosphere. In fact, the factor  $PGM/(\kappa R^2 \tau)$  is altered by  $f_P$  (Eq. 9).  $f_P$  was taken as a constant over the whole atmosphere, its value being the same as the outermost point of the envelope.

The above expressions are valid only for conservative potentials. As the model evolves the resulting potential is no longer

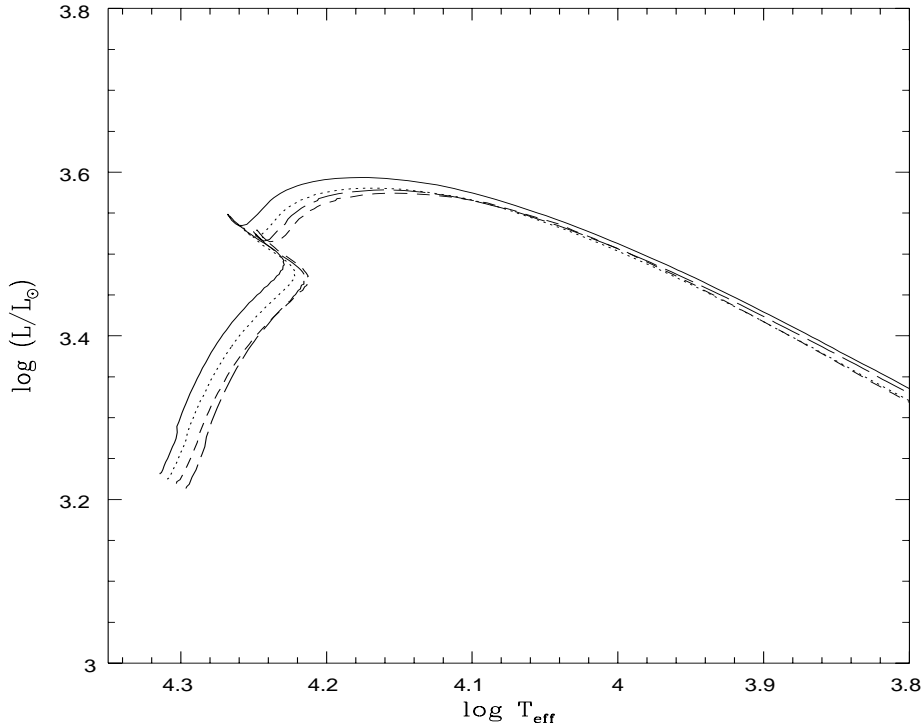


**Fig. 1.** Standard and rotating models ( $7 M_{\odot}$ ). Continuous line indicates a model without rotation, long dashed rotating model with  $\Omega_i = 8.5 \times 10^{-5} s^{-1}$ , small dashed line denotes model with  $\Omega_i = 7 \times 10^{-5} s^{-1}$  and dotted line represents a model with  $\Omega_i = 5 \times 10^{-5} s^{-1}$ . For sake of clarity only these three rotating models are shown. Case 1.

conservative and the density and temperature are not constant on equipotentials if local conservation of angular momentum is adopted. Meynet & Maeder 1997 indicated under which conditions the set of equations proposed by KT can be used in such cases (the equations are written in terms of isobars and the density is substituted by an average value over neighboring isobars instead over equipotentials). We do not expect large differences between the present treatment and the more elaborated proposed by Meynet & Maeder, at least for not excessively distorted configurations.

In order to simplify the treatment of the redistribution of angular momentum two simple laws were selected:

1. rigid body, where the angular velocity is the same throughout the model
2. local conservation of angular momentum.

The first law means that the redistribution of the angular momentum is complete, while for the second law there is no redistribution. Surely a redistribution of angular momentum between these mentioned limits is more realistic. In fact, the evolution of the angular velocity must be obtained through integration of a fourth order differential equation which depends, among other variables, on the circulation speed (Zahn 1992 and for practical application, see Talon et al. 1997). The assumption of local conservation of angular momentum produces  $\Omega$  profiles much more pronounced than in the case where the corresponding differential equation is integrated. This probably may yields to a wrong interpretation of the effects of rotation. Adopting the two mentioned laws, we do not consider transport of angular momentum due to rotationally-induced instabilities. The induced mixing is governed by a diffusion equation – coupled with the differential equation for the evolution of the angular velocity

– and is important for the transport of angular momentum as well as for the whole evolution of a rotating star. These remarks surely limit our conclusions but do not invalidate them. A more detailed investigation on induced mixing is under progress.

Provided that the angular velocity is far from the critical one, the model converges after a few iterations. The angular momentum distribution is stored in order to evaluate the distribution of angular velocity for the following models. The total conservation of the angular momentum is controlled by integrating the individual contribution of each shell. For example, the differences between the initial model and that at the end of hydrogen shell-burning is very small and of the order of 0.0001% and it is probably due to redistribution of points in the interior of the models during evolution.

Disregarding the prescriptions of angular momentum redistribution, the initial model is supposed to rotate as a rigid body. Up to 3000 shells are used in each individual model. The number of points in the envelope is around 500. As the apsidal motion is detected in moderate and massive stars our reference models have 2, 7 and  $15 M_{\odot}$ . A sequence of about 350 models were generated for each mass and for each angular momentum prescription with different values of the initial angular velocities. The main properties of such models will be discussed in the next section.

### 3. Discussion of the results and conclusions

The computation of the models was stopped when the critical angular velocity was reached (if this occurs). Almost all the models were well below this limiting value. As in general the results indicated a similar behaviour of the rotating models with respect to the non rotating counterparts, we restrict our discus-

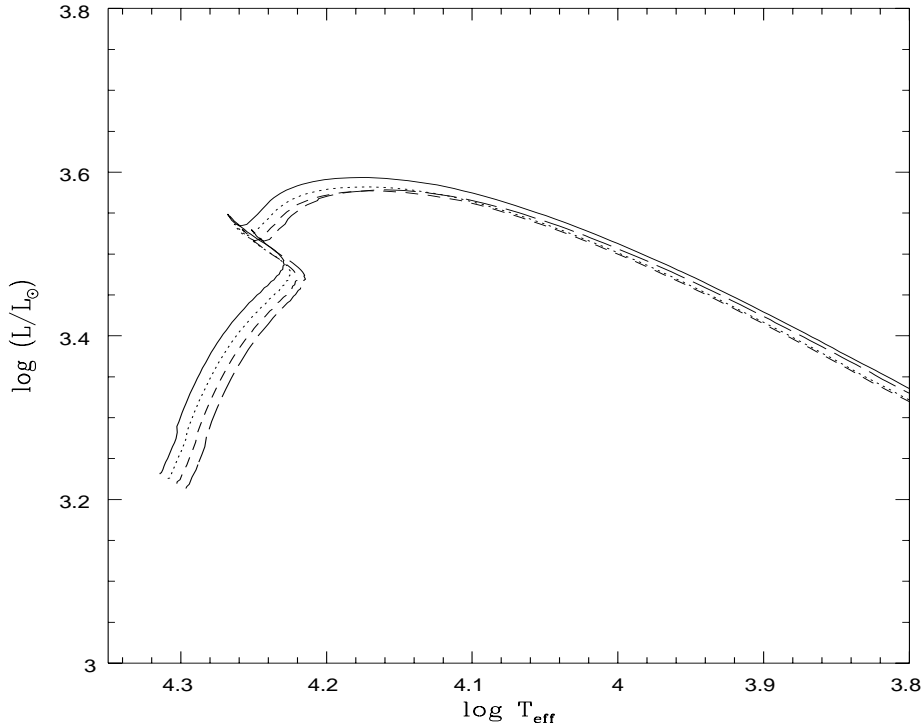


**Fig. 2.** Standard and rotating models. The same legend as in Fig. 1. Case 2.

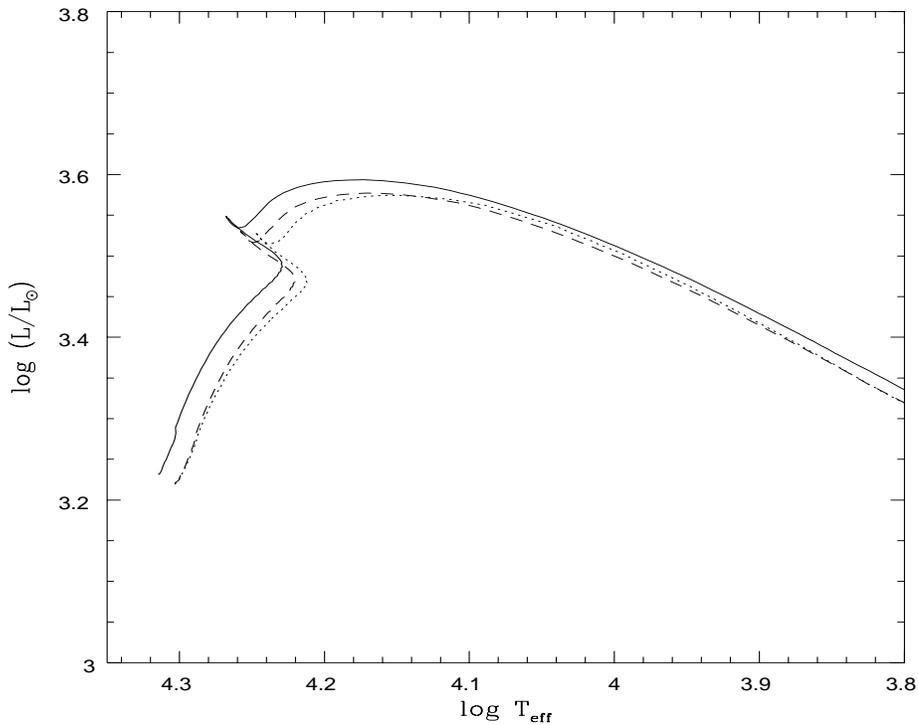


**Fig. 3.** More detailed comparison between rotating models in Case 1 (dotted line) and 2 (long dashed line) for  $\Omega_i = 7 \times 10^{-5}$ .

sion fundamentally to the  $7 M_{\odot}$  model. In Fig. 1 we can see the comparative HR diagram for rotating and non rotating models for  $7 M_{\odot}$  (Case 1). The adopted chemical composition was  $(X, Y) = (0.70, 0.28)$  with a mixing-length parameter  $\alpha=1.52$ . Core overshooting has not been considered, neither mass loss, to make more evident the effects of rotation. The classical effect of luminosity and effective temperature lowering is clearly seen as well as the dependence of these deviations on the initial

angular momentum. Five values of the initial angular velocities  $\Omega_i$ , say, 2, 4, 5, 7 and  $8.5 \times 10^{-4} \text{ s}^{-1}$  were used, though only three cases were plotted.

For models with local conservation of angular momentum (same  $\Omega_i$ ) the situation is similar (Fig. 2) but with some differences as one can see with more detail in Fig. 3, which shows the corresponding non rotating model and two rotating models with the same  $\Omega_i$  but computed following the two laws of angular

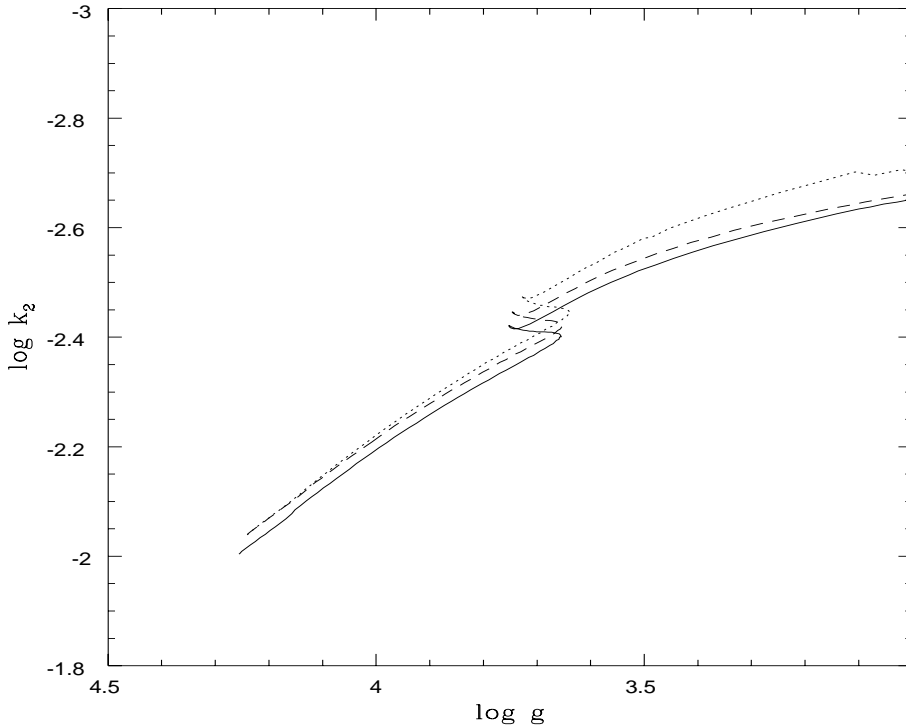


**Fig. 4.** The apsidal motion constant for the same models shown in Fig. 3

momentum redistribution. Generally speaking, we can say that rotating models computed under the assumption of rigid body rotation are more distorted in the surface than its counterpart of Case 2. Keeping in mind that the shape of the equipotential surfaces is given by Eq. 2, a simple mathematical analysis permits us to conclude that the variation of  $f_P$  and  $f_T$  with the radius depends on how  $f_2$  varies with radial distance. For Case 1 the interior of the model will not be excessively distorted in the central regions ( $f_P$  and  $f_T$  almost equal to 1) while for the outermost layers these values are substantially smaller, depending on the assumed  $\Omega_i$ . On the other hand, the situation is just the opposite for differentially rotating models since the equipotential surfaces in the centre are well distorted while they are almost spherical in the surface of the model. As it was assumed that all initial models rotate like a rigid body, the differences between both models in Fig. 3 are not large, at least for the first models. However, as the models evolve, these differences increase as a consequence of the above arguments.

Concerning the apsidal motion constant, Fig. 4 shows the behaviour of the three models shown in Fig. 3. The correction for rotation (measured at the same  $\log g$ ) in  $\log k_2$  is around  $-0.05$  for slightly evolved models, which is within the estimation made by Claret & Giménez 1993 for ZAMS models. The models computed under Case 2 are always between the standard model and the rotating one following prescription 1. At the end of the hydrogen burning phase, the differences increase and for more evolved configurations the difference can reach approximately  $-0.15$  for Case 1. The differences in mass concentration with respect to a non rotating model for Case 2 is almost constant over the plane  $\log g \times \log k_2$  and the mean correction is of the order of  $-0.05$ . The gyration radius is slightly changed by

rotation. It is smaller by around 2% with respect to non rotating models.

In order to see with more detail how  $k_2$  depends on the evolutionary stage, on the initial angular momentum and on the assumed redistribution law, Fig. 5 shows the results for three significant phases, say,  $X_c=0.70, 0.35$  and the redest point during the Main-Sequence as a function of  $\Omega_i$ . As expected, for small values of the initial rotation and/or for early stages, there is no significant alterations in the models. As already mentioned, the differences in  $\log k_2$  between Case 1 and Case 2 increase with evolution, for a fixed  $\Omega_i$ .

The results shown in Fig. 5 are interesting but it is hard to compare them directly with observational data. Indeed, we do not have observational data on the initial angular velocities and how angular momentum is redistributed during evolution. Although we do not know  $\Omega_i$  under the observational point of view, it is possible to get another important parameter to evaluate the effects of rotation:  $\lambda$ , computed at the surface. Such a variable gives a measure of the ratio of the centrifugal to gravitational force, and therefore, of the distortion of the rotating models. In Fig. 6 we plot the differences in  $\log k_2$  between rotating and standard models as a function of  $\lambda_s$ . The selected points correspond to 3 different masses, two different laws of redistribution, several evolutive phases and different values of  $\Omega_i$ . It is very interesting to note that, disregarding all these mixed conditions, the correction for rotation can be approximated by a straight line, with a good level of confidence. This feature was already pointed out by Sothers 1974 and Claret & Giménez 1993 but only for ZAMS models. The average slope is  $-0.87$ , that is,  $\delta \log k_2 = -0.87 \lambda_s + 0.004$ . This value is very similar to that obtained by the three mentioned authors. To understand

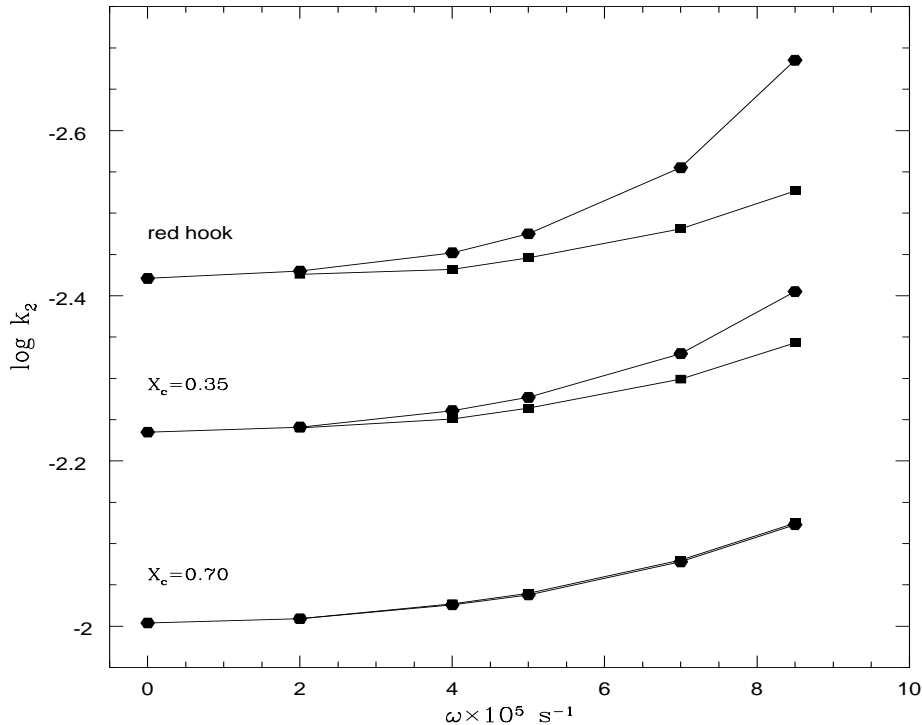


**Fig. 5.** Effect of the magnitude and redistribution law of angular momentum on  $\log k_2$  for the same models shown in Figs. 1 and 2. Filled hexagons indicate models with rigid body rotation (Case 1) and filled squares denote rotating models with local conservation of angular momentum (Case 2). The curves beginning at  $\Omega_i = 0$  describe the deviations with respect to no rotating model for  $X_c = 0.70, 0.35$  and for the red hook point, respectively.

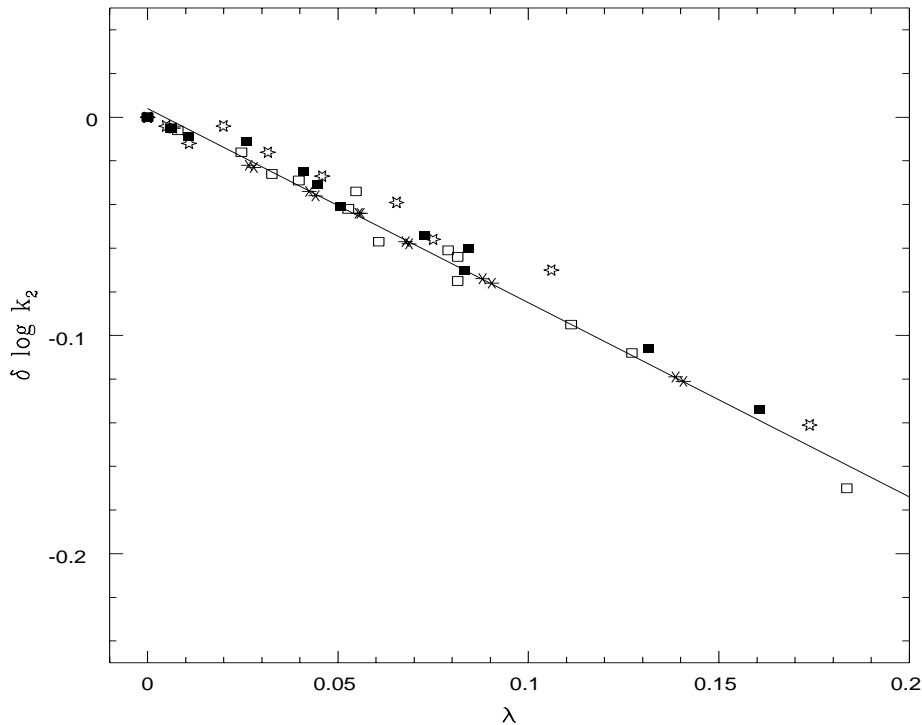


**Fig. 6.** The correction for rotation as a function of  $\lambda$ , computed at the surface for models of 2, 7 and 15  $M_\odot$ . Some significant evolutionary phases are represented assuming several angular momentum values and the two redistribution laws. Asterisks represent models with  $X_c=0.70$ , open squares models with  $X_c=0.35$ , models at the red hook are denoted by solid squares while stars represent models at the hydrogen shell-burning.

this simple relationship, let us write  $\lambda_s$  as  $2\Omega_s^2 R^3 / (3GM)$ . For centrally condensed configurations, the surface value of  $\eta_2$  is around 3 and thus,  $\lambda_s$  is directly connected with  $f_2$  that defines the degree of distortion of a given model. In other words, the more distorted is the model the more the apsidal motion constant deviates from the standard value at the same evolutionary

stage. Similar relationships can also be inferred as a function of the difference between the gravities, at the same evolutionary status, for rotating and standard models.

Summarizing, the present results indicate that there is a direct and linear relation between how much the star is distorted and how its internal structure changes, particularly the apsidal

motion constant. We have found that the influence of rotation on internal structure depends strongly on the distortion of the configuration characterized by the parameter  $\lambda_s$ . Such results make the work of introducing the correction for rotation in the apsidal motion analysis an easier task since it is sufficient to reduce the theoretical  $\log k_2$  by  $0.87 \lambda_s$ . Fig. 10 by Claret & Giménez 1993 shows the discrepancies between  $\log k_{obs}$  and  $\log k_{theo}$  for a sample of eclipsing binaries as a function of  $\lambda$  at the surface. Such figure suggests an approximately linear relationship between these parameters. However, these results should be taken with care since there are points which represent stars with good, mean and poor absolute dimension determinations. The asterisks in that figure denote the systems with high accuracy in their absolute dimensions and they define a slope compatible with that obtained theoretically here. The additional systems define a larger slope. Given their mean errors in the masses and radii it is not wise to draw conclusions rashly.

A final remark: as commented, the adopted simplifications pointed out in Sect. 2 may restrict our conclusions mainly for very faster rotators. The effects of the rotational induced instabilities on the internal structure of stars and their connection to dynamical evolution of close binary stars will be matter of a future paper.

*Acknowledgements.* The Spanish DGYCIT (PB96-0840) is gratefully acknowledged for support during the development of this work.

## References

- Cisneros-Parra J.U., 1970, A&A 8, 141  
 Claret A., 1995, A&AS 109, 441  
 Claret A., 1997, A&A 327, 11  
 Claret A., 1998, A&A 330, 533  
 Claret A., 1999, A&A, in press  
 Claret A., Giménez A., 1992, A&AS 96, 255  
 Claret A., Giménez A., 1993, A&A 277, 487  
 Endal A.S., Sofia S., 1976, ApJ 210, 184  
 Faulkner J., Roxburgh I.W., Strittmatter P.A., 1968, ApJ 152, 203  
 Iglesias C.A., Rogers F.J., Wilson B.G., 1992, ApJ 397, 771  
 Hejlesen P.M., 1987, A&AS 69, 251  
 Kippenhahn R., Thomas R.C., 1970, In: Slettebak A. (ed.) Stellar Rotation. D. Reidel Publ. Co., Dordrecht, Holland, p. 20  
 Koch R.H., 1972, PASP 84, 5  
 Kopal Z., 1959, Close Binary Systems. Chapman & Hall, London  
 Kopal Z., 1965, Advances in Astronomy and Astrophysics 3, 89  
 Mathis J.S., 1967 ApJ 149, 619  
 Meynet G., Maeder A., 1997, A&A 321, 465  
 Moffat J.W., 1984, ApJ 287, L77  
 Moffat J.W., 1989, Phys. Rev. D 39, 474  
 Petty A.F., 1973, Ap&SS 21, 189  
 Randers G., 1942, ApJ 95, 454  
 Rogers R.J., Iglesias C.A., 1992, ApJS 79, 507  
 Schwarzschild M., 1958, Structure and Evolution of the Stars. Dover Publ., New York  
 Semeniuk I., Paczynski B., 1968, Acta Astron. 18, 33  
 Stothers R., 1974, ApJ 194, 651  
 Talon S., Zahn J.-P., Maeder A., Meynet G. 1997, A&A 322, 209  
 Zahn J.-P., 1992, A&A 265, 115